DMD Fast Forward. Published on September 21, 2007 as doi:10.1124/dmd.107.016998

TITLE PAGE

In vitro metabolism study of combretastatin A-4 in rat and human liver microsomes

Silvio Aprile, Erika Del Grosso, Gian Cesare Tron and Giorgio Grosa

Dipartimento di Scienze Chimiche, Alimentari, Farmaceutiche e Farmacologiche and Drug and Food Biotechnology Center, Università degli Studi del Piemonte Orientale "A. Avogadro", Largo Donegani 2, 28100 Novara, Italy.

RUNNING TITLE PAGE

a) Combretastatin A-4 *in vitro* metabolism.

b) Corresponding author:

Giorgio Grosa - Dipartimento di Scienze Chimiche, Alimentari, Farmaceutiche e Farmacologiche and Drug and Food Biotechnology Center, Università degli Studi del Piemonte Orientale "A. Avogadro", Largo Donegani 2, 28100 Novara, Italy.

tel +39 (0)321 375854 Fax 39 (0)321 375621

e-mail: grosa@pharm.unipmn.it

c)

Text pages : 35

Tables : 1

Figures : 6

References: 24

Abstract: 233 words

Introduction: 436 words

Discussion: 863 words

d) Non-standard abbreviations list:

APT: attached proton test; **CA-4:** *(Z)*-combretastatin A-4; **DAD:** diode array detector; **DMF:** N,N-dimethylformamide; **ESI:** electrospray ionization; **MS/MS:** tandem mass spectrometry; **NOE:** Nuclear Overhauser Effect; **PDC:** pyridinium dichromate; **TBAF:** tetrabutylammonium fluoride; **TBDMSCl:** *t*-butyldimethylsilyl chloride.

DMD Fast Forward. Published on September 21, 2007 as DOI: 10.1124/dmd.107.016998
This article has not been copyedited and formatted. The final version may differ from this version.

ABSTRACT

The phase I biotransformation of combretastatin A-4 (CA-4) **1**, a potent tubulin polymerization inhibitor with antivascular and antitumoral properties, was studied using rat and human liver subcellular fractions. The metabolites were separated by HPLC and detected with simultaneous UV and ESI mass spectrometry. The assignment of metabolite structures was based on ESI-MS/MS experiments and confirmed by comparison with reference samples obtained by synthesis.

O-demethylation and aromatic hydroxylation are the two major phase I biotransformation pathways, the latter being regioselective for phenyl ring B of **1**. Indeed, incubation with rat and human microsomal fractions led to the formation of a number of metabolites, seven of which were identified. The regioselectivity of microsomal oxidation was also demonstrated by the lack of metabolites arising from stilbenic double bond epoxidation. Alongside the oxidative metabolism, *Z*-*E* isomerization during *in vitro* study was also observed contributing to the complexity of the metabolite pattern. Moreover, when **1** was incubated with a cytosolic fraction, metabolites were not observed. Aromatic hydroxylation at the C-6' of phenyl ring B and isomerization led to the formation of M1 and M2 metabolites which were further oxidized to the corresponding *para*-quinone (M7 and M8) species whose role in pharmacodynamic activity is unknown. Metabolites M4 and M5, arising from *O*-demethylation of phenyl ring B, did not form the *ortho*-quinones. *O*-demethylation of phenyl ring A formed the metabolite M3 with a complete isomerization of the stilbenic double bond.

INTRODUCTION

The combretastatins are a large family of natural products extracted from *Combretum caffrum* (Pettit et al., 1987; Pettit et al., 1989). In particular, combretastatin A-4 (CA-4); (*Z*)-3'-hydroxy-3,4,4',5-tetramethoxy-stilbene) **1** (figure 1) is the most potent of these compounds. In the original manuscripts, **1** was described as a strong cell growth and tubulin inhibitor (Lin et al., 1988; Pettit et al., 1989). These features, ultimately, induced the disruption of microtubular function (McGown and Fox, 1989) causing the selective and irreversible damage to the neovasculature of tumors. Because of its poor solubility in water, a more soluble pro-drug, CA-4 phosphate (CA-4-P) **2**, has been developed as the selected lead for *in vivo* and human studies. (Mealy et al.,2006). **1** is not the only molecule of the family to have entered clinical trials. AVE8062 **3**, a synthetic analogue bearing a different substitution on ring B, has recently done so as well (Lippert, 2006). Indeed, combretastatin A-1 phosphate (Oxi4503) **4** which retains the same biological and structural signature, has been shown to possess features that should make it suitable for therapeutic intervention (Lippert, 2006). Treatment with **2**, which is rapidly converted by non-specific endogenous phosphatases, present in plasma and in endothelial cells, to the active compound **1** (Pettit et al., 1995), disrupts selectively the tumoral vasculature causing reduction of the blood flow within the tumor and subsequent massive hemorrhagic necrosis (Tozer et al., 1999; Grosios et al., 1999). These results have been demonstrated at doses less than one-tenth of the maximum tolerated (Dark et al., 1997), in contrast with other structurally related tubulin-binding agents (*e.g.* vincristine, vinblastine podophyllotoxin and colchicine). The pharmacokinetics of **2** has also been investigated during preclinical and clinical studies (Rustin et al., 2003; Stevenson et al., 2003; Kirwan et al., 2004), while no data are available for the metabolic fate of **1**. Stratford *et al.* (Stratford et al., 1999), postulated the presence of combretastatin A-4 metabolites without determining their structures. Similarly, Kirwan *et al.* (Kirwan et al., 2004), stated that the metabolic profile of the drug is complex, but also in this case no effort was made to identify the metabolites.

Finally, Rustin *et al.* (Rustin et al., 2003), in their phase I clinical study, confirmed the rapid transformation of **2** into the active **1** and reported the formation of the CA-4 glucuronide.

These considerations linked to our interest in the medicinal chemistry of CA-4 **1** (Tron et al., 2006), led us to study the metabolic fate of **1** in rat and human microsomal preparations. In the present paper, the major *in vitro* phase I biotransformation pathways of **1** with the formation of quinonic species is described.

DMD Fast Forward. Published on September 21, 2007 as DOI: 10.1124/dmd.107.016998
This article has not been copyedited and formatted. The final version may differ from this version.

METHODS

Reagents and chemicals.

Methanol (HPLC grade), acetonitrile (HPLC grade) were purchased from Sigma–Aldrich (Milano, Italy). Water (HPLC grade) was obtained from Milli-Q RO system. Titriplex®V, Extrelut®3 and Extrelut®1 columns were purchased from Merck (Darmstadt, Germany). 3,4-dihydroxybenzaldehyde, 2,4,5-trimethoxybenzaldehyde, Aliquat 336, boron tribromide (1 M in dichloromethane), butyllithium (1.6 M in tetrahydrofuran), diisopropylethylamine, dimethyl sulfate, Fremy's salt (potassium nitrosodisulfonate), imidazole, iodine, lithium aluminium hydride, PDC, sodium hydride (60%), TBAF (1M in tetrahydrofuran), TBDMSCl, trifluoroacetic acid were used without further purification and were purchased from Sigma-Aldrich. (Milano, Italy). Tetrahydrofuran (THF) was dried over lithium aluminium hydride to remove peroxides and stored on activated molecular sieves (4Å). DMF and dichloromethane were dried and stored on activated molecular sieves (4Å). When needed, the reactions were performed in oven-dried glassware under a positive pressure of dry N_2. Column chromatography was performed on silica gel (Merck Kieselgel 70-230 mesh ASTM) using the indicated eluants. Thin layer chromatography (TLC) was carried out on plates with a layer thickness of 0.25 mm (Merck silica gel 60 F254). Melting points were determined in an open glass capillary with a Stuart scientific SMP3 apparatus and are uncorrected.

The following compounds were prepared according to literature procedures:

CA-4 **1** and *(E)*-combretastatin A-4 (Gaukroger et al., 2001); 3,4,5-trimethoxybenzyltriphenylphosphonium bromide **6** (Kong et al., 2005); 2,3-dihydroxy-4-methoxy-benzaldehyde **20** (Kaisalo et al., 1986); 3,5-dihydroxy-4-methoxy-benzoic acid methyl ester **12** (Cardona et al., 1986).

DMD Fast Forward. Published on September 21, 2007 as DOI: 10.1124/dmd.107.016998
This article has not been copyedited and formatted. The final version may differ from this version.

Instrumentation and chromatographic conditions.

LC-DAD-UV.

A Shimadzu HPLC system, with two LC-10AD *Vp* module pumps, an SLC-10A *Vp* system controller and a DGU-14-A on-line degasser, was used for the analysis. The chromatographic separations were performed on a *Phenomenex Luna 5µ C18(2) (250 x4.6 mm)* as the stationary phase protected by a C18-Security Guard™. A model 7725i Rheodyne valve was used for the injection of samples (20 µL). The SPD-M10Avp photodiode array detector was used to detect the analytes at 330 nm. A ClassVp 5.03 software was used to process the chromatograms. The isocratic mobile phase (flow rate 1.0 mL/min) consisted in water/acetonitrile 60:40 (v/v) (0.5% formic acid) mixture. The eluants were filtered through a 0.45 µm pore size PVDF membrane filter prior the use. All of analyses were carried out at room temperature.

LC-ESI-MS.

A Thermo Finningan LCQ Deca XP *plus* system equipped with a quaternary pump, a Surveyor AS autosampler and a vacuum degasser was used for LC-MS analysis. The chromatographic separation was performed on a *Phenomenex Luna 5µ C18(2) (250 x4.6 mm)* as the stationary phase protected by a Security Guard™ C18. The sample injection volume was 20 µL. The eluate was injected into the electrospray ion source (ESI) with a splitting of 20% and MS/MS spectra were acquired and processed using Xcalibur® software.

Operating conditions on the ion trap mass spectrometer in positive ion mode were as follows: spray voltage, 3.50 kV; source current, 80 µA; capillary temperature, 350 °C; capillary voltage, 11.60 V; tube lens offset, 5 V; multipole 1 offset, -7.00 V; multipole 2 offset, -8.50 V; sheath gas flow (N_2), 60 A.U. Data were acquired in MS/MS product ion scan mode using mass scan range m/z 90-400 and the collision energy was optimized at 32%.

DMD Fast Forward. Published on September 21, 2007 as DOI: 10.1124/dmd.107.016998
This article has not been copyedited and formatted. The final version may differ from this version.

^{1}H /^{13}C NMR.

^{1}H and ^{13}C APT and NOE experiments were performed on a JEOL ECP 300 FT MHz spectrophotometer. Chemical shifts are reported in part per million (ppm).

Rat liver cytosol and microsomes.

Male Wistar rat liver microsomes (protein concentration: 22.5 mg/mL, total CYP 0.64 nmol/mg protein) and cytosol (protein concentration: 11.5 mg/mL,) were used throughout this study and prepared using the previously described protocol (Grosa et al., 2004). The rat liver microsomal CYP concentration was determined by the method of Omura and Sato (Omura and Sato, 1964).

Incubations were performed using an horizontal DUBNOFF shaking thermostatic bath.

Rat liver fractions incubation.

The standard incubation mixture, in 10 mL polyethylene tubes, contained 1.3 mM $MgCl_2 \cdot 6H_2O$, 0.4 mM $NADPNa_2$, 3.6 mM glucose 6-phosphate, 0.4 Units/mL glucose 6-phosphate dehydrogenase in a 0.1 M phosphate buffer, pH 7.4, containing 1.5 mM Titriplex®V (an ethylenediamine tetra-acetic acid analogue), 0.84 mg/mL of surfactant Tween 80 and 1mM CA-4, brought to a final volume of 3 mL. After pre-equilibration of the mixture, an appropriate volume of microsomal suspension or cytosol was added to give a final protein concentration of 1 mg/mL or 1.5 mg/mL for microsomal suspensions or cytosol respectively; the mixture was shaken for 60 minutes at 37°C. Control incubations were done without the NADPH-regenerating system or with boiled microsomes. The incubation mixtures were then extracted on Extrelut®3 using 15 mL of chloroform/ethyl acetate/2-propanol 45:45:10 as eluant. The organic phase was evaporated under reduced pressure and the crude extract was reconstituted in acetonitrile (0.5 mL) and analysed by LC-DAD-UV and LC-ESI-MS.

DMD Fast Forward. Published on September 21, 2007 as DOI: 10.1124/dmd.107.016998
This article has not been copyedited and formatted. The final version may differ from this version.

Human liver fractions incubation.

Cryopreserved CYPreme™ Human Liver Microsomes (pooled mixed sex, ten individuals donors, protein concentration: 21 mg/mL, total CYP: 0.476 nmol/mg) were purchased from InVitro Technologies GmbH (Leipzig, Germany) and used throughout this study.

All the operations were performed protected from the light. To maximally exploit the activity of the human liver microsomes the conditions suggested by the supplier were adopted. Hence, the standard incubation mixture, in Eppendorf tubes, contained 0.6 mM $NADPNa_2$, 6.4 mM glucose 6-phosphate, 1.5 Units/mL glucose 6-phosphate dehydrogenase, 60 mM $NaHCO_3$ in a 0.1 M phosphate buffer, pH 7.4, containing 1.5 mM Titriplex®V, 10 µL of acetonitrile (1% of incubation total volume) and 38 µM or 100 µM CA-4, brought to a final volume of 1 mL. After pre-equilibration of the mixture, an appropriate volume of microsomal suspension was added to give a final protein concentration of 1 mg/mL; the mixture was shaken in air for 60 min at 37°C. Control incubations were done without the NADPH-regenerating system. The incubation mixtures were then extracted on Extrelut®1 using 6 mL of chloroform/ethyl acetate/2-propanol 45:45:10 as eluant. The organic phase was evaporated under reduced pressure and the crude extract was reconstituted with acetonitrile (150 µL) and analysed by LC-DAD-UV and LC-ESI-MS.

Synthesis of putative metabolites.

Synthesis of (E)-3',4-dihydroxy- 3,4',5-trimethoxy-stilbene 5.

1 (254 mg, 0.8 mmol) was dissolved in dichloromethane (2.5 mL) and cooled to –78°C. Boron tribromide (1M solution in dichloromethane, 0.8 mL) was added dropwise under magnetic stirring. After completion of the reaction, ethyl acetate was added and the mixture was neutralized with saturated $NaHCO_3$ solution. The organic layer was washed with brine, dried over anhydrous Na_2SO_4, filtered and evaporated under reduced pressure. The residue was purified by column

DMD Fast Forward. Published on September 21, 2007 as DOI: 10.1124/dmd.107.016998
This article has not been copyedited and formatted. The final version may differ from this version.

chromatography using petroleum ether/ethyl acetate 7:3 and then 6:4 as eluants to give compound **5**, (46 mg, 19% yield).

^{1}H-NMR *(300 MHz, $CDCl_3$) δ 7.1(d, J=2.2 Hz, H-2'), 6.9(dd, J=8.2/2.2 Hz, H-6'), 6.87(s, 2H), 6.82(d, J=8.2 Hz, H-5'), 6.7(s, 2H), 5.6(s, OH), 5.5(s, OH), 3.94(s, 2OCH_3), 3.90(s, OCH_3).*

^{13}C-NMR *(300 MHz, $CDCl_3$) δ 147.2(2C ring A), 146.3(C), 145.8(C), 134.5(C), 131.2(C), 129.2(C), 127.3(CH), 126.5(CH), 119.1(CH), 111.6(CH), 110.7(CH), 103.1(2CH ring A), 56.4(2OCH_3), 56.3(OCH_3).*

MS(ESI) *m/z 303 $[M+H]^+$.*

UV *(CH_3CN) λ_{max}: 245, 335 nm.*

Synthesis of (Z)-3',4'-dihydroxy-3,4,5-trimethoxy-stilbene 10 and (E)-3',4'-dihydroxy-3,4,5-trimethoxy-stilbene 11.

3,4-dihydroxybenzaldehyde (2 g, 14 mmol) and diisopropylethylamine (7.36 mL, 42 mmol) were dissolved in dry DMF (20 mL). The resulting solution was cooled to 0°C and TBDMSCl (6.48 g, 43 mmol) was added. After completion of the reaction the mixture was diluted with ethyl acetate and neutralized with 2N HCl. The organic layer was washed with brine, dried over anhydrous Na_2SO_4, filtered and evaporated under reduced pressure.

The residue was purified by column chromatography using petroleum ether/ethyl acetate (95:5 and then 9:1) as eluant to give 3,4-di[(*t*-butyldimethylsilyl)oxy]benzaldehyde **7** (4.73 g, 93% yield).

Under a N_2 atmosphere, the phosphonium salt **6** (2.9 g, 6.5 mmol) was dissolved in dry THF (15 mL) and the suspension was cooled to –15°C. Sodium hydride 60%, (545 mg, 13.6 mmol) was then added. The reaction mixture was stirred for 1 h until the solution became red. Subsequently, compound **7** (2 g, 5.5 mmol), dissolved in dry THF (10 mL), was added dropwise and the reaction was stirred overnight. The mixture was diluted with ethyl acetate and neutralized with 2N HCl. The organic layer was washed with brine, dried over anhydrous Na_2SO_4, filtered and evaporated under reduced pressure. The residue was purified by column chromatography using petroleum ether/ethyl

acetate 99:1 as eluant to give: (*Z*)-3',4'-di[(*t*-butyldimethylsilyl)oxy]-3,4,5-trimethoxy-stilbene **8**, (115 mg), (*E*)-3',4'-di[(*t*-butyldimethylsilyl)oxy]-3,4,5-trimethoxy-stilbene **9**, (167 mg) and 1.96 g as mixture of the two isomers; total yield 78%. Compound **8**, (115 mg, 0.2 mmol) was dissolved in dry THF (2.5 mL). A solution of TBAF was added (1M in tetrahydrofuran, 440µL). After completion of the reaction the mixture was diluted with dichloromethane and washed with water. The organic layer was washed with brine, dried over anhydrous Na_2SO_4, filtered and evaporated under reduced pressure. The residue was purified by column chromatography using petroleum ether/ethyl acetate 8:2 and then 6:4 as eluants to give compound **10** (24 mg, 36% yield).

Starting from compound **9** (167 mg, 0.3 mmol) compound **11** (56 mg, 61 % yield) was obtained using the conditions used for **10**.

Compound **10**;

^{1}H-NMR *(300 MHz, $CDCl_3$) δ 6.8(s, H), 6.74(s, H), 6.73(s, H), 6.5(s, 2H), 6.4(d, J=12.1 Hz, H-olefinic), 6.3(d, J=12.1 Hz, H-olefinic), 4.8(broad peak 2OH), 3.8(s, OCH_3), 3.6 (s, $2OCH_3$).*

MS(ESI) *303 $[M+H]^+$.*

UV *(CH_3CN) λ_{max}: 245, 300 (broad) nm.*

Compound **11**;

^{1}H-NMR *(300 MHz, $CDCl_3$) δ 7.0(s, broad H-2'), 6.91(dd, J=7.95/1.6 Hz, H-6' overlapped with 6.88), 6.88(d, J=15 Hz, 1H-olefinic), 6.85(d, J=7.95 Hz, overlapped with 6.88, H-5'), 6.83(d, J=16.2 Hz, 1H-olefinic), 6.6(s, 2H), 6.3(broad peak 2OH), 3.87(s, $2OCH_3$), 3.86(s, OCH_3).*

MS(ESI) *m/z 303 $[M+H]^+$.*

UV *(CH_3CN) λ_{max}: 245, 335 nm.*

Synthesis of 3,5-di[(t-butyldimethylsilyl)oxy]-4-methoxy-benzoic acid methyl ester 13.

Compound **12**, (1.5 g, 7.6 mmol) and imidazole (2.6 g, 38 mmol) were dissolved in dry DMF (26 mL). The resulting solution was cooled to 0°C and TBDMSCl (2.8 g, 19 mmol) was added. The mixture was stirred overnight at room temperature. The reaction was worked up by dilution with

DMD Fast Forward. Published on September 21, 2007 as DOI: 10.1124/dmd.107.016998
This article has not been copyedited and formatted. The final version may differ from this version.

diethyl ether. The organic layer was washed with 2N HCl and brine. After drying over anhydrous Na_2SO_4, filtration and evaporation of the solvent gave a colourless oil **13** (3.2 g, 98% yield) which was used directly without further purification.

^{1}H-NMR *(300 MHz, $CDCl_3$) δ 7.2(s, 2H), 3.9(s, interchangeable signal OCH_3), 3.8(s, interchangeable signal OCH_3), 1.0(s, $2SiC(CH_3)_3$), 0.2(s, $2Si(CH_3)_2$).*

Synthesis of 3,5-di[(t-butyldimethylsilyl)oxy]-4-methoxy-benzyl alcohol 14.

Compound **13**, (3.2 g, 7.5 mmol) was dissolved in diethylether (32 mL) and the solution was cooled to 0°C. Lithium aluminium hydride (0.6 g, 16 mmol) was added in small portions under magnetic stirring. After an hour, the mixture was treated with silica gel (4.8 g) and saturated NH_4Cl solution. The mixture was filtered through a pad of Celite® and washed with diethylether. The filtrate was washed with brine, dried over anhydrous Na_2SO_4, filtered and evaporated under reduced pressure to give compound **14** as a viscous colourless oil (2.9 g, 98% yield) which was used directly without further purification.

^{1}H-NMR *(300 MHz, $CDCl_3$) δ 6.5(s, 2H), 4.5(s, CH_2OH), 3.7(s, OCH_3), 1.0(s, $2SiC(CH_3)_3$), 0.2(s, $2Si(CH_3)_2$).*

Synthesis of 3,5-di[(t-butyldimethylsilyl)oxy]-4-methoxy-benzaldehyde 15.

To a solution of compound **14**, (2.9 g, 7.3 mmol) in dichloromethane (30 mL), PDC (3.8 g, 10 mmol) was added and the mixture stirred for 12 h.

The reaction was worked up by dilution with dichloromethane. The organic layer was washed with 2N HCl, brine and was dried over Na_2SO_4 and filtered. Evaporation of the solvent gave a crude product which was purified by column chromatography using petroleum ether/ethyl acetate 98:2 to give compound **15** as a white solid (1.8 g, 70% yield).

^{1}H-NMR *(300 MHz, $CDCl_3$) δ 9.8(s, CHO), 7.0(s, 2H), 3.8(s, OCH_3), 1.0(s, $2SiC(CH_3)_3$), 0.2(s, $2Si(CH_3)_2$).*

Synthesis of (Z)-3',5'-di[(t-butyldimethylsilyl)oxy]-3,4,4',5-tetramethoxy-stilbene 16.

Under a N_2 atmosphere, phosphonium salt **6**, (1.0 g, 2.3 mmol) was dissolved in dry THF (10 mL). The solution was cooled to –15°C and butyllithium (1.6 M solution in tetrahydrofuran, 1.8 mL) was added. The reaction mixture was stirred until the solution became red. Subsequently compound **15**, (0.9 g, 2.3 mmol) dissolved in dry THF (7 mL) was added dropwise and stirred at room temperature for 1 h. The mixture was diluted with ethyl acetate and neutralized with saturated NH_4Cl solution. The organic layer was washed with brine, dried over anhydrous Na_2SO_4, filtered and evaporated under reduced pressure. The residue was purified by column chromatography using petroleum ether/ethyl acetate 95:5 as eluant to give in order: compound **16** (*Z*) pure (0.5 g, 37% yield), and then 0.4 g of mixture (*Z+E)* compounds both as yellow oils.

^{1}H-NMR *(300 MHz, $CDCl_3$) δ 6.4(m, broad 4H), 6.3(s, 2H), 3.8(s, OCH_3), 3.7(s, $2OCH_3$), 3.6(s, OCH_3), 0.9(s, $2SiC(CH_3)_3$), 0.1(s, $2Si(CH_3)_2$).*

Synthesis of (Z)-3'5'-dihydroxy-3,4,4',5-tetramethoxy-stilbene 17.

Compound **16**, (80 mg, 0.14 mmol) was dissolved at 0°C in dry THF (1 mL). TBAF was added (1M in tetrahydrofuran, 300 µL). After 1 h, the reaction mixture, which rapidly developed an intense dark red colour, was neutralized with cold 2N HCl and extracted with ethyl acetate. The organic layer was washed with brine, dried over anhydrous Na_2SO_4, filtered and evaporated under reduced pressure. The residue was purified by column chromatography using petroleum ether/ethyl acetate 6:4 as eluant to give compound **17**, (46 mg, 98% yield) as a white solid.

^{1}H-NMR *(300 MHz, $CDCl_3$) δ 6.5(s, 2H), 6.45(s, 2H), 6.41(s, 2H), 5.4(s, broad 2OH), 3.84(s, OCH_3), 3.82(s, OCH_3), 3.6(s, $2OCH_3$).*

MS(ESI) *m/z 333 $[M+H]^+$.*

UV *(CH_3CN) λ_{max}: 240, 295 (broad) nm.*

DMD Fast Forward. Published on September 21, 2007 as DOI: 10.1124/dmd.107.016998
This article has not been copyedited and formatted. The final version may differ from this version.

Synthesis of (E)-3',5'-di[(t-butyldimethylsilyl)oxy]-3,4,4',5-tetramethoxy-stilbene 18.

Compound **16**, (0.2 g, 0.4 mmol) was dissolved in chloroform (9 mL), and iodine, (29 mg, 0.1 mmol) was added. The mixture was stirred at room temperature for 14 h. The reaction was worked up by dilution with chloroform and washed with a saturated solution of $Na_2S_2O_4$. The organic layer was washed with brine, dried over anhydrous Na_2SO_4, filtered and evaporated under reduced pressure. The residue was purified by column chromatography using petroleum ether/ethyl acetate 9:1 as eluant to give compound **18**, (37 mg, 21% yield) as a white solid.

^{1}H-NMR *(300 MHz, $CDCl_3$) δ 6.8(m, broad 4H), 6.6(s, 2H), 3.9(s, 2OCH_3), 3.8(s, OCH_3), 3.7(s, OCH_3), 1.0(s, 2$SiC(CH_3)_3$), 0.2(s, 2$Si(CH_3)_2$).*

Synthesis of (E)-3',5'-dihydroxy-3,4,4',5-tetramethoxy-stilbene 19.

Starting from compound **18** (37 mg, 0.06 mmol) and with the same procedure used for **17**, compound **19** (14 mg, 64 % yield) was obtained as a yellow oil.

^{1}H-NMR *(300 MHz, $CDCl_3$) δ 6.9(d, J=16.2 Hz, H-olefinic), 6.8(d, J=15.9 Hz, H-olefinic), 6.69(s, 2H), 6.67(s 2H), 3.9(s, 4OCH_3).*

MS(ESI) *m/z 333 $[M+H]^+$.*

UV *(CH_3CN) λ_{max}: 245, 330 nm.*

Synthesis 2,3-di[(t-butyldimethylsilyl)oxy]-4-methoxy-benzaldehyde 21.

Compound **20**, (1.2 g, 7.1 mmol) and diisopropylethylamine (3.8 mL, 22 mmol) were dissolved in dry DMF (12 mL) and stirred at 0°C. TBDMSCl (3.3 g, 22 mmol) was added. After 30 minutes, the mixture was filtered through a pad of Celite® washed with water and then with ethyl acetate. The organic layer was neutralized with 2N HCl, washed with brine, dried over anhydrous Na_2SO_4, filtered and evaporated under reduced pressure.

The residue was purified by column chromatography using petroleum ether/ethyl acetate 95:5 as eluant to give compound **21**, (1.9 g, 67% yield).

^{1}H-NMR *(300 MHz, $CDCl_3$) δ 10.2(s, CHO), 7.4(d, J=8.8 Hz, H), 6.6(d, J=8.8 Hz, H), 3.8(s, OCH_3), 1.0(s, $SiC(CH_3)_3$), 0.9(s $SiC(CH_3)_3$), 0.1(s, $2Si(CH_3)_2$).*

Synthesis of (Z/E)-2',3'-dihydroxy-3,4,4',5-tetramethoxy-stilbene 22.

Under a N_2 atmosphere, the phosphonium salt **6**, (0.1 g, 0.22 mmol) was dissolved in dry THF (1 mL) and the solution was cooled at –15°C. Butyllithium solution (0.2 mL) (1.6 M in tetrahydrofuran) was then added. The reaction mixture was stirred until the solution became red. Subsequently, compound **21** (0.1 g, 0.25 mmol), dissolved in dry THF (1 mL), was added dropwise and the reaction mixture was stirred at room temperature for 30 minutes. The mixture was diluted with ethyl acetate and neutralized with a saturated NH_4Cl solution. The organic layer was washed with brine, dried over anhydrous Na_2SO_4, filtered and evaporated under reduced pressure. The residue was purified by column chromatography using petroleum ether/ethyl acetate 9:1 as eluant to give (*Z/E*)-2',3'-di[(*t*-butyldimethylsilyl)oxy]-3,4,4',5-tetramethoxy-stilbene, compound **22 (**mixture of isomers) as a pale brown oil (70 mg, 49% yield). Compounds **22**, (70 mg, 0.18 mmol) were dissolved at 0°C in dry THF (2 mL) and TBAF was added (1M in tetrahydrofuran, 300 µL). After completion of the reaction the mixture was neutralized with cold 2N HCl and extracted with ethyl acetate. All organic layers were washed with brine, dried over anhydrous Na_2SO_4, filtered and evaporated under reduced pressure. The residue was purified by column chromatography using petroleum ether/ethyl acetate 7:3 as eluant to give compound **23 (**mixture of isomers), (30 mg, 73% yield) as a yellow oil.

MS(ESI) *m/z 333 $[M+H]^+$.*

UV *(CH_3CN)* **(*Z*)** *λ_{max}: 240, 300 (broad) nm,* **(*E*)** *λ_{max}: 245, 330 nm.*

Synthesis of 2,5-dihydroxy-4-methoxy-benzaldehyde 24.

Under a N_2 atmosphere, 2,4,5-trimethoxybenzaldehyde, (10 g, 51 mmol) was dissolved in dry dichloromethane (150 mL) and the resulting solution was cooled to –10°C. Boron tribromide (1M

in dichloromethane, 75 mL) was slowly added and then after two hours the reaction was quenched by addition of a saturated $NaHCO_3$ solution. The organic layer was dried over anhydrous Na_2SO_4, filtered and partially evaporated under reduced pressure. After cooling to 4°C a crystalline precipitate **24** (319 mg, 3.7% yield) was formed and collected.

m.p. *204.8 °C; melting point literature 209°C* (Daly et al., 1961).

^{1}H-NMR *(300 MHz, DMSO-d_6) δ 10.5(s, CHO), 9.9(s, OH), 8.9(s, OH), 7.0(s, H-6), 6.5(s, H-3), 3.8(s, OCH_3).*

MS(ESI) *m/z 169 $[M+H]^+$.*

Synthesis of 2,5-di[(t-butyldimethylsilyl)oxy]-4-methoxy-benzaldehyde 25.

Compound **24**, (243 mg, 1.4 mmol) and imidazole (490 mg, 7.2 mmol) were dissolved in dry DMF (10 mL) and the reaction mixture was cooled to 0°C. TBDMSCl (650 mg, 4.3 mmol) was added and the reaction was stirred overnight at room temperature. The mixture was diluted with ethyl acetate and washed with 1N HCl, brine and dried over anhydrous Na_2SO_4. Filtration and evaporation of the solvent gave a residue which was purified by column chromatography using initially, petroleum ether and then petroleum ether/ethyl acetate 9:1 as eluants to give compound **25**, (490 mg, 85% yield) as a white solid.

^{1}H-NMR *(300 MHz, $CDCl_3$) δ 10.2(s, CHO), 7.2(s, H), 6.2(s, H), 3.8(s, OCH_3), 0.99(s, $SiC(CH_3)_3$), 0.97(s, $SiC(CH_3)_3$), 0.2(s, $Si(CH_3)_2$), 0.1(s, $Si(CH_3)_2$).*

Synthesis of (Z)-2'5'-di[(t-butyldimethylsilyl)oxy]-3,4,4',5-tetramethoxy-stilbene 26, and (E)-2'5'-di[(t-butyldimethylsilyl)oxy]-3,4,4',5-tetramethoxy-stilbene 27.

Under a N_2 atmosphere, phosphonium salt **6** (1.2 g, 2.7 mmol) was dissolved in dry THF (20 mL) and the reaction mixture was cooled at –15°C. Butyllithium (1.6 M in tetrahydrofuran, 1.7 mL) was added until the solution became red. Subsequently compound **25**, (880 mg, 2.2 mmol) dissolved in dry THF (20 mL), was added dropwise and stirred at room temperature for 6 h. The mixture was

diluted with ethyl acetate and neutralized with saturated NH_4Cl solution. The organic layer was washed with brine, dried over anhydrous Na_2SO_4, filtered and evaporated under reduced pressure. The residue was purified by column chromatography using petroleum ether/ethyl acetate 99:1 as eluant to give compounds: **26** (*Z*), 30 mg, **27** (*E*), 35 mg and a mixture of isomers (*Z*+*E*), 419 mg. Total yield 39%.

Compound **26**;

^{1}H-NMR *(300 MHz, $CDCl_3$) δ 6.6(s, H), 6.57(d, J=11.9 Hz, H-olefinic), 6.50(s, 2H), 6.4(d, J=11.9 Hz, H –olefinic), 6.3(s, H), 3.8(s, OCH_3), 3.74(s, OCH_3), 3.70(s, $2OCH_3$), 1.0(s, $SiC(CH_3)_3$), 0.8(s, $SiC(CH_3)_3$), 0.2 (s, $Si(CH_3)_2$), -0.02 (s, $Si(CH_3)_2$).*

^{13}C-NMR *(300 MHz, $CDCl_3$) δ 153.0(2C), 150.8(C), 148.2(C), 139.2(C), 137.1(C), 133.3(C), 128.4(CH), 126.1(CH), 121.5(CH), 120.4(C), 105.9(2CH), 104.6(CH), 60.9(OCH_3), 55.9($2OCH_3$), 55.6(OCH_3), 25.9($SiC(CH_3)_3$), 25.6($SiC(CH_3)_3$), 18.3(2SiC), -4.0($Si(CH_3)_2$) -4.8($Si(CH_3)_2$).*

Compound **27**;

^{1}H-NMR *(300 MHz, $CDCl_3$) δ 7.33(d, J=16.2 Hz, H-olefinic), 7.0(s, H), 6.77(d, J=16.2 Hz, H-olefinic), 6.71(s, 2H overlapped with 6.77), 6.3(s, H), 3.89(s, $2OCH_3$), 3.86(s, OCH_3), 3.7(s, OCH_3), 1.06(s, $SiC(CH_3)_3$), 1.01(s, $SiC(CH_3)_3$), 0.2(s, $Si(CH_3)_2$), 0.1(s, $Si(CH_3)_2$).*

^{13}C-NMR *(300 MHz, $CDCl_3$) δ 153.4(2C), 151.1(C), 147.8(C), 139.7(C), 137.4(C), 134.0(C), 125.6(CH), 122.9(CH), 120.6(C), 116.9(CH), 104.5(CH), 103.0(2CH), 61.0(OCH_3), 56.0($2OCH_3$), 55.5(OCH_3), 25.8(2$SiC(CH_3)_3$), 18.4(SiC), 17.3(SiC), -4.1($Si(CH_3)_2$), -4.5 ($Si(CH_3)_2$).*

Synthesis of (E)-2-methoxy-5-[2-(3,4,5-trimethoxy-phenyl)-vinyl]-[1,4]benzoquinone 28.

Method A

To a solution of a mixture of compounds **26**, **27** (100 mg, 0.18 mmol) in dry peroxide free THF (3 mL), TBAF (1M in tetrahydrofuran, 356 µL) was added at 0°C. After 1 h, the reaction mixture, which rapidly developed an intense dark red colour, was diluted with ethyl acetate and neutralized with 1N HCl. The organic layer was washed with brine, dried over anhydrous Na_2SO_4, and after

DMD Fast Forward. Published on September 21, 2007 as DOI: 10.1124/dmd.107.016998
This article has not been copyedited and formatted. The final version may differ from this version.

filtration evaporated under reduced pressure. The crude product was purified by column chromatography using petroleum ether/ethyl acetate 6:4 as eluant to give compound **28**, (39 mg, 67% yield).

Method B

To a mixture of Aliquat 336 (91 µL) and $NaH_2PO_4 \bullet H_2O$ (162 mg, 1.17 mmol) in water (50 mL), a solution of *(E)*-combretastatin A-4 (50 mg, 0.16 mmol) dissolved in dichloromethane (3.5 mL) was added. Then, Fremy's salt (potassium nitrosodisulfonate) (106 mg, 0.40 mmol) was added and the mixture was stirred for 1h (the colour changes from mauve to red).

The reaction was worked up by dilution with dichloromethane and washed with water. The aqueous layer was further washed with dichloromethane, and the combined organic extracts were washed with brine. After drying over Na_2SO_4, filtration and evaporation of the solvent, the crude product was purified by column chromatography using petroleum ether/ethyl acetate 7:3 as eluant to give compound **28**, (19 mg, 38% yield).

^{1}H-NMR *(300 MHz, $CDCl_3$) δ 7.3(d, J=16,2 Hz, H-olefinic), 7.0(d, J=16.5 Hz, H-olefinic),6.8 (s, H-quinone, meta to OCH_3), 6.7(s, 2H), 5.9(s, H-quinone, ortho to OCH_3), 3.9(s, $2OCH_3$), 3.87(s, OCH_3), 3.84(s, OCH_3).*

^{13}C-NMR *(300 MHz, $CDCl_3$) δ 187.1(CO), 182.1(CO), 159.2(C), 153.5(2C), 142.6(C), 139.8(C), 138.3(CH), 131.7(C), 125.3(CH), 118.5(CH), 107.4(CH), 104.9(2CH), 61.1(OCH_3), 56.4(OCH_3), 5.3($2OCH_3$).*

MS(ESI) *m/z 331 $[M+H]^+$.*

UV *(CH_3CN) λ_{max}: 235, 295 (broad) nm.*

Synthesis of (Z)-2-methoxy-5-[2-(3,4,5-trimethoxy-phenyl)-vinyl]-[1,4]benzoquinone 29.

To a mixture of Aliquat 336 (91 µL) and $NaH_2PO_4 \bullet H_2O$ (162 mg, 1.17 mmol) in water (50 mL), a solution of **1** (50 mg, 0.16 mmol) dissolved in dichloromethane (3.5 mL) was added. Then, Fremy's

DMD Fast Forward. Published on September 21, 2007 as DOI: 10.1124/dmd.107.016998
This article has not been copyedited and formatted. The final version may differ from this version.

salt (potassium nitrosodisulfonate) (106 mg, 0.40 mmol) was added and the mixture was stirred for 30 minutes (the colour changes from mauve to red).

The reaction was worked up by dilution with dichloromethane and washed with water. The aqueous layer was further washed with dichloromethane, and the combined organic extracts were washed with brine. After drying over Na_2SO_4, filtration and evaporation of the solvent, the crude product was purified by column chromatography using petroleum ether/ethyl acetate 65:35 as eluant to give compound **29**, (17 mg, 31 % yield).

^{1}H-NMR *(300 MHz, $CDCl_3$) δ 6.9(d, J=12,2 Hz, H-olefinic), 6.7(s, H-quinone, meta to OCH_3), 6.5(s, 2H), 6.4(dd, J=12.5/1.2 Hz, H-olefinic next to quinone ring), 5.9(s, H-quinone, ortho to OCH_3), 3.85(s, OCH_3), 3.82(s, OCH_3), 3.7(s, $2OCH_3$).*

^{13}C-NMR *(300 MHz, $CDCl_3$) δ 187.2(CO), 182.2(CO), 158.7(C), 153.5(2C), 143.1(C), 142.5(C), 138.8(CH), 131.2(C), 130.0(CH), 120.4(CH), 107.5(CH), 105.7(2CH), 61.8(OCH_3), 56.3(OCH_3), 56.2($2OCH_3$).*

MS(ESI) *m/z 331 $[M+H]^+$.*

UV (CH_3CN) λ_{max}: 235, 275 (broad) nm.

Synthesis of (Z)-2'5'-dihydroxy-3,4,4',5-tetramethoxy stilbene 30.

To a solution of compounds 26 and 27 (mixture) (265 mg, 0.47 mmol) in THF (10 mL) and methanol (20 mL), cooled to 0°C, 20 mL of trifluoroacetic acid (67% aqueous solution) were added. The reaction was stirred for 5 h and than diluted with ethyl acetate and neutralized with saturated Na_2CO_3 solution. The organic layer was washed with brine, dried over anhydrous Na_2SO_4, filtered and evaporated under reduced pressure. The residue was purified by column chromatography using petroleum ether/ethyl acetate 6:4 as eluant to give compound to give compound 30, (7 mg, 4.5% yield).

DMD Fast Forward. Published on September 21, 2007 as DOI: 10.1124/dmd.107.016998
This article has not been copyedited and formatted. The final version may differ from this version.

^{1}H-NMR *(300 MHz, $CDCl_3$) δ 6.7(s, H), 6.6(d, J=11.9 Hz, H-olefinic), 6.50(s, 2H), 6.45(s, overlapped with 6.44, H), 6.44(d, J=11.9 Hz, H-olefinic), 5.2(s, broad OH), 4.7(s, broad OH), 3.83(s, OCH_3), 3.81(s, OCH_3), 3.6(s, $2OCH_3$).*

^{13}C-NMR *(300 MHz, $CDCl_3$) δ 153.0(2C), 146.9(C), 146.0(C), 139.4(C), 137.8(C), 132.1(CH), 131.4(C), 123.8(CH), 115.5(C), 114.4(CH), 105.7(2CH), 99.6(CH), 60.9(OCH_3), 56.1(OCH_3), 55.9($2OCH_3$).*

ESI-MS *m/z 333 $[M+H]^+$.*

UV *(CH_3CN) λ_{max}: 235, 290 (broad), 330 (broad) nm.*

Synthesis of (E)-2'5'-dihydroxy-3,4,4',5-tetramethoxy stilbene 31.

To a solution of **28**, (39 mg, 0.12 mmol) in diethylether (2 mL), an excess of an aqueous $Na_2S_2O_4$ solution was added under vigorous magnetic stirring. After 30 minutes, when the colour changed from dark-red to yellow, the aqueous layer was removed and the organic layer was evaporated under reduced pressure to give compound **31**, (32 mg, 80% yield).

^{1}H-NMR *(300 MHz, $CDCl_3$) δ 7.1(d, J=16.2 Hz, H-olefinic), 7.0(s, H), 6.8(d, J=16.2 Hz, H-olefinic), 6.7(s, 2H), 6.4(s, H), 3.88(s, $2OCH_3$), 3.85(s, OCH_3), 3.84(s, OCH_3).*

^{13}C-NMR *(300 MHz, $CDCl_3$) δ 153.3(2C), 146.8(C), 141.5(C), 139.8(C), 137.5(C), 133.6(C), 128.2(CH), 122.0(CH), 117.0(C), 111.6(CH), 103.3(2CH), 100.2(CH), 61.1(OCH_3), 56.1(OCH_3), 56.0($2OCH_3$).*

ESI-MS *m/z 333 $[M+H]^+$.*

UV (CH_3CN) λ_{max}: 245, 295, 350 nm.

DMD Fast Forward. Published on September 21, 2007 as DOI: 10.1124/dmd.107.016998
This article has not been copyedited and formatted. The final version may differ from this version.

RESULTS

Synthesis of putative metabolites.

The Wittig reaction was used for the preparation of the putative metabolites **10**, **11**, **17**, **19**, **23**, **28**, **29**, **30**, **31**. Indeed, appropriate protected aldehydes and phosphonium salt intermediates were prepared and reacted to obtain the *Z/E* mixture of combretastatin analogues.

Compound **5** was easily prepared by selective demethylation using boron tribromide. (scheme 1 supplemental data); it is worth mentioning that the reaction occurred with complete *Z-E* isomerization of the double bond. The synthesis of **10** and **11** were performed by reacting compounds **7** and **6** (scheme 2 supplemental data). The *E* and *Z* isomers were separated by column chromatography and subsequently deprotected in the presence of TBAF. The Wittig reaction with **15** and the phosphonium salt **6** provided the *Z* isomer **16** and a *Z/E* mixture of isomers which could not be separated by column chromatography to give the pure *E* isomer. Compound **17** was easily obtained by deprotection of **16**. (scheme 3 supplemental data). The *E* isomer **19** was prepared starting from **16** by using I_2 induced isomerization (Gaukroger et al., 2001) and deprotection with TBAF. The synthesis of the putative metabolites **23** required the preparation of aldehyde intermediate **21** which was subsequently reacted with phosphonium salt **6** to give **22** as a *Z/E* mixture which could not be separated by column chromatography (scheme 4 supplemental data). For this reason, after deprotection, compound **23** was obtained as a 1:1 mixture. Chromatographic separation of two geometric isomers *Z/E* of compound **23** was achieved from elution into LC-DAD-UV system. Compounds **30** and **31** were obtained starting from 2,4,5-trimethoxy benzaldehyde which was selectively demethylated to **24** by BBr_3 treatment. To establish the correct structure, NOE was performed by selective irradiation of the methoxy group, resulting in NOE enhancement (3.3%) of the singlet signal at 6.5 ppm (scheme 5 supplemental data). The protected aldehyde intermediate **25** was then reacted with phosphonium salt **6** to give **26** and **27**. TBAF deprotection of the isomeric mixture only resulted in the formation of the *E*-quinonic compound **28**. The reduced

form **31** was obtained by reacting **28** in the presence of sodium dithionite. The *Z* isomer **30** was obtained starting from the isomeric mixture of **26** and **27** which was deprotected by using trifluoroacetic acid to give both compounds **30** and **31** separated by column chromatography.

Compounds **28**, **29** and **30**, **31** were also prepared in a more convenient and straightforward way by using Fremy's salt as a biomimetic oxidant. Indeed the reaction of **1** with Fremy's salt in a heterogeneous system (water/dichloromethane) and in the presence of Aliquat 336, as a phase transfer catalyst, afforded the quinone **29** which was easily reduced with sodium dithionite to **30**. The same procedure was also used to obtain compounds **28** and **31** starting from *E*-CA-4.

In vitro CA-4 metabolism in rat and human liver microsomes.

1 was incubated in rat and human liver microsomal fractions in the presence of a NADPH-regenerating system. Because of the lipophilic character of the drug, Tween-80 or acetonitrile (<1% v/v) were used to increase the solubility in the incubation medium: no difference was observed in the metabolite pattern. In order to enhance the formation of metabolites, 1mM of **1** was used through rat study. Indeed, when a lower concentration (100 μM) was used, no significant differences in the metabolite pattern were observed. Metabolites were recovered from incubation media by a liquid-liquid extraction on Extrelut® columns.

LC-DAD-UV analysis of rat and human microsomal incubations.

1 and its metabolites were separated by HPLC using a C-18 reverse-phase column and a mixture of H_2O/CH_3CN acidified with 0.5% formic acid as eluant. The LC-DAD-UV analysis of rat liver microsome incubations (figure 2A) showed the presence of at least eight metabolites (M1-M8) which were not observed in incubations performed in the absence of the NADPH-regenerating system (figure 2C). Moreover, any metabolic transformation occurred when **1** was incubated with boiled microsomes or with the cytosolic fraction. The analysis of human liver microsome incubations, as reported in figure 2B, afforded a very similar metabolic pattern to that observed with

rat liver preparations. The DAD-UV analysis of the chromatographic peaks of rat liver incubations allowed us to assign the geometric isomerism to metabolites M1-M8. Indeed, it has been reported that UV data are of relevance to characterize the geometric isomerism of stilbene derivatives (Yu et al., 2002). In particular, **1** showed two absorbance maxima at 245 and 300 nm, while a batochromic shift to 330 nm was observed for the *E*-isomer (figure 3). Consequently, *Z* and *E* configurations were attributed to the M5-M6 and M3-M4 metabolites respectively (figure 1 supplemental data).

The UV spectra of M1, M2, M7 and M8 showed a slightly different absorbance pattern suggesting a more marked modification of the stilbenic scaffold. In particular M1 and M2 spectra were characterized by three absorbance maxima; however, batochromic shifts (275-295 nm for M8 and 330-350 nm for M2) were again observed, allowing us to assign the *E* configuration to M2 and M8 and *Z* configuration to M1 and M7.

LC-ESI-MS/MS analysis of rat microsomal incubation.

In order to obtain further information on the M1-M8 structures, positive LC-ESI-MS/MS analyses of the incubations with rat microsomes were performed. The structural features of **1** suggest that the metabolites could arise from three putative metabolic pathways: *O*-demethylation, aromatic hydroxylation and epoxidation. Indeed, the LC-ESI-MS analysis performed in ion positive MS/MS mode (303 *m/z*) allowed the detection of *O*-demethylated metabolites (figure 4). In particular, the peaks appearing at 14.13, 15.25, 18.36 and 20.40 minutes correspond to M3, M4, M5 and M6 peaks in the UV-traces. The MS/MS experiments demonstrated the presence of a similar fragmentation pattern for these metabolites (table 1). Nonetheless, these data are not sufficient to correctly assign their structures. Hence, the CA-4 *O*-demethylated analogues: *(E)*-3',4-dihydroxy- 3,4',5-trimethoxy-stilbene **5**, *(Z)*-3',4'-dihydroxy-3,4,5-trimethoxy-stilbene **10** and *(E)*-3',4'-dihydroxy-3,4,5-trimethoxy-stilbene **11** were synthesized. The chromatographic properties, the mass spectrometry and UV data for **5**, **11** and **10** completely matched with those of M3, M4, M5 respectively. Possibly, M6 could also arise from *O*-demethylation of one of the two *meta* methoxy groups at the positions

DMD Fast Forward. Published on September 21, 2007 as DOI: 10.1124/dmd.107.016998
This article has not been copyedited and formatted. The final version may differ from this version.

C-3 and C-5 on phenyl ring A of **1**. To detect the metabolites arising from aromatic hydroxylation, LC-ESI-MS analysis was performed in ion positive MS/MS mode (333 *m/z*) (figure 4). The peaks detected at 10.71 and 11.87 min corresponded to metabolites M1 and M2; MS/MS experiments revealed a very similar fragmentation pattern (table 1): this feature, together with UV data suggest that the metabolites were isomers. All of the positional isomers, *(Z)* and *(E)*-3',5'-dihydroxy-3,4,4',5-tetramethoxy-stilbene **17**, **19** respectively, *(Z/E)*-2',3'-dihydroxy-3,4,4',5-tetramethoxy-stilbene **23**, *(Z)* and *(E)*-2'5'-dihydroxy-3,4,4',5-tetramethoxy-stilbene **30**, **31** were synthesized. In particular, compounds **30** and **31** showed the same chromatographic, mass spectral and UV properties as metabolites M1 and M2. The presence of catechol and *para*-hydroquinone moieties in the M4, M5 and the M1, M2 structures respectively, suggest the possible formation of the corresponding *ortho* and *para*-quinone species in incubation medium. Indeed LC-ESI-MS analysis performed in ion positive MS/MS mode (331 *m/z*) revealed two peaks at 22.58 and 31.15 (figure 4) which correspond to metabolites M7 and M8 in the UV-traces. The pseudomolecular ion $[M+H]^+$at 331 *m/z*, the fragmentation patterns and the UV properties allowed us to assign a quinone structure to M7 and M8. The synthesis of isomers **29** and **28** confirmed the assigned structures. On the contrary, metabolites arising from the oxidation of the catechol function (M4, M5) were not found.

LC-ESI-MS/MS analysis of human microsomal incubation.

LC-ESI-MS/MS analysis of the human microsomal incubation extracts, reported in Figure 5, confirmed the presence of metabolites M1-M8 and the complexity of metabolic fate of **1**. Hence, as previously shown by UV-traces, the metabolite pattern was similar to that obtained from rat microsomal incubations except that the unknown M6 metabolite was apparently the more abundant metabolite arising from the *O*-demethylation pathway; indeed M3, M4 and M5 were only formed in low amounts. Even if a reference standard corresponding to M6 was not synthetized, however the structure of *(Z)*-3,3'-dihydroxy-4,4',5-trimethoxy-stilbene could be proposed for this metabolite. Indeed the *O*-demethylation of **1** at the C-4 and C-4' methoxy functions resulted in the formation of

M3 and M4, M5 respectively. Hence, the only other *O*-demethylation pathway should occur at one of the two *meta* methoxy groups on ring A. Interestingly M6 shows the typical UV-spectrum of a *Z*-stilbene derivative (Figure1 supplemental data) being different with that of M3. Possibly the metabolic *O*-demethylation pathway occurred with or without olefin bond isomerization depending on the position of the methoxy group. The formation of M1 and M2 as well as the related quinone metabolites M7 and M8 was also observed (Figure 5, MS/MS 331 m/z). Finally two other peaks at 20.51 and 24.55 minutes were observed in the LC-MS trace (Figure 5, MS/MS 331) which having the same MS/MS data obtained from M7 and M8 should be attributed to another couple of quinone metabolites. In theory, the quinone metabolites could arise from the related catechols obtained by aromatic hydroxylation at C-2' and C-6'. In particular the *ortho*-quinone of ring B could be formed from the corresponding catechol with the same structure of CA-1. However chromatographic, MS/MS and UV data of both geometric isomers of CA-1, synthesized as reference standard **23** were not detected in human LC-MS trace possibly indicating their ready oxidation to the quinone species.

DISCUSSION

Up to now, the oxidative biotransformation of combretastatin A-4 has not been studied; hence an *in vitro* study of metabolic stability in the presence of rat and human liver subcellular preparations was undertaken. In order to maximize the metabolite formation from **1,** rat liver incubations were performed at 1 mM substrate concentration. It is worthwhile to note that the incubations in the presence of a lower concentration (100 μM) did not show significant qualitative differences. On the other hand, for the study with human liver microsomes a 38 μM concentration of **1** was used. Indeed in the clinical studies the administered dose of CA-4 phosphate was in the range 52-68 mg/m^2 affording a plasma concentration of CA-4 phosphate and **1** of 30.3-46.3 and 1.9-2.3 μM respectively (Dowlati et al., 2002; Rustin et al, 2003). Rationally, a 2 μM substrate concentration would have been ideal for our study. However the obtained results with rat liver incubations suggested that this concentration was too low to detect the metabolites preventing also the determination of geometric isomerism by DAD-UV on-column analysis. These considerations led us to choose an about twentyfold greater concentration similar to that achieved in plasma by the CA-4 phosphate prodrug. The *in vitro* human and rat hepatic microsomal metabolism of **1** involves two main metabolic pathways (figure 6): *O*-demethylation and aromatic hydroxylation. In particular, aromatic hydroxylation was observed only on phenyl ring B. The steric hindrance of the trimethoxy substituents possibly prevented the hydroxylation on phenyl ring A and, in this case, only an *O*-demethylation pathway was observed. *O*-demethylation on ring B affords two isomeric catechol metabolites M4 and M5. Interestingly, the metabolic *O*-demethylation of **1** to M3 and M4 occurred with isomerization of the olefin bond. On the contrary in human microsomes, the *Z*-*E* conversion was not observed during the formation of M6. Initially, we thought that the formation of metabolites with *E* configuration could be attributed to the transformation of *E*-CA-4 present in small amounts (<2%) in our **1** sample. However this hypothesis was ruled out because when pure *E*-CA-4 was incubated with rat liver microsomes, only two metabolites were formed (data not shown);

DMD Fast Forward. Published on September 21, 2007 as DOI: 10.1124/dmd.107.016998
This article has not been copyedited and formatted. The final version may differ from this version.

moreover the percentage of the *E*-isomer in metabolites was greater than that of *E*-CA-4 present in our *Z*-CA-4. Finally, a stability study of **1** in phosphate buffer, using the same conditions applied in the incubations showed only a small isomerization. These data suggest the *Z-E* isomerization of the olefin bond occurred mainly during metabolic *O*-demethylation as well as aromatic hydroxylation of **1.** In particular the isomerization seems to occur when a *para*-methoxy group was demethylated both on ring A and B, while it did not when the methoxy group was in *meta* position. Actually**,** no study has been performed on this topic, hence from the available data a mechanism of isomerization could not be assumed. Metabolites M4 and M5 were characterized by a catechol function whose oxidation to *ortho*-quinone is a well known metabolic pathway for various classes of compounds (i.e. estrogens, polycyclic aromatic hydrocarbon), however *ortho*-quinones related to M4 and M5 were not detected in **1** incubations. On the contrary, metabolites M1 and M2, arising from the aromatic hydroxylation of ring B were easily oxidized to the corresponding *para*-quinone metabolites M7 and M8 both in rat and human microsomes. This oxidative step might be catalyzed by monooxygenase or peroxidase enzymes but also by metal ions and molecular oxygen. It is worth mentioning that the mass spectral data obtained from human liver incubation extracts suggested the possible formation of other quinone metabolites. Indeed, two catecholic metabolites could arise from the aromatic hydroxylation at C-2' and C-6'. In particular, the metabolic hydroxylation at C-2' and concurrent isomerization could form both geometric isomers of CA-1 whose oxidation generated the related *ortho*-quinone metabolites. Generally, quinones represent a class of toxic intermediates which can create a variety of harmful effects through differents mechanism (Bolton et al., 2000). However, in a study on CA-1, a hydroxylated analog of CA-4, Kirwan *et al.* postulated that the marked antitumor activity of CA-1 may be due to the formation of a reactive *ortho*-quinone metabolite (Kirwan et al. 2004). Nonetheless no conclusive evidence was obtained about the metabolic formation of the CA-1 related quinone metabolite. Moreover the relevance of the quinone species of **1** in *in vivo* metabolism could also depend on other metabolic pathways like the glucuronidation and the reduction by DT diaphorase. Taken together these considerations suggest

that the role of quinone metabolites in the pharmacodynamics of combretastatins remains to be established.

Overall the metabolic profile of CA-4 did not show significant differences in incubation with rat and human microsomes except that the metabolite M6 was more abundant in human preparations and that the presence of other putative quinone metabolites was revealed. Hence we propose the following *in vitro* metabolic scheme (figure 6), where **1** undergoes oxidative biotransformation in rat and human microsomes leading to an array of metabolites characterized by both *E* and *Z* configurations. The formation of *para*-quinone metabolites was also unequivocably demonstrated. Further work will be necessary to completely assess the structure-metabolism relationship of the combretastatins A-4 and A-1 and the relevance of their quinone metabolites in the pharmacokinetic and pharmacodynamic phases.

ACKNOWLEDGEMENTS

Richard Billinghton is kindly acknowledged for the revision of the manuscript.

REFERENCES

Bolton JL, Trush MA, Penning TM, Dryhurst G, Monks TJ (2000) Role of Quinones in Toxicology. *Chem. Res. Tox.* **13:** 135-160.

Cardona ML, Fernandez MI, Garcia MB, Pedro JR (1986) Synthesis of natural polyhydroxystilbenes. *Tetrahedron*, **42:** 2725-30.

Daly J, Horner L, Witkop B (1961) Chemical and Enzymatic Routes to Methoxydopamines. *J. Am. Chem. Soc.* **83:** 4787-4791.

Dowlati A, Robertson K, Cooney M, Petros WP, Stratford M, Jesberger J, Rafie N, Overmoyer B, Makkar V, Stambler B, Taylor A, Waas J, Lewin JS, McCrae KR, Scot, Remick SC (2002) A Phase I Pharmacokinetic and Translational Study of the Novel Vascular Targeting Agent Combretastatin A-4 Phosphate on a Single-Dose Intravenous Schedule in Patients with Advanced Cancer. *Cancer Res.* **62:** 3408-3416.

Gaukroger K, Hadfield JA, Hepworth LA, Lawrence NJ, McGown AT (2001) Novel Syntheses of Cis and Trans Isomers of Combretastatin A-4 *J. Org. Chem.* **66:** 8135-8138.

Grosa G, Galli U, Rolando B, Fruttero R, Gervasio G, Gasco A (2004) Identification of 2,3-diaminophenazine and of o-benzoquinone dioxime as the major *in vitro* metabolites of benzofuroxan. *Xenobiotica* **34:** 345–352.

Grosios K, Holwell SE, McGown AT, Pettit GR, Bibby MC (1999) *In vivo* and *in vitro* evaluation of combretastatin-A4 and its sodium phosphate prodrug. *Br. J. Cancer* **81:** 1318-1327.

Kaisalo L, Latvala A, Hase T (1986) Selective Demethylations in 2,3,4-trimethoxyaryl carbonyl compounds. *Synthetic Comm.* **16:** 645-8.

Kirwan IG, Loadman PM, Swaine DJ, Antoney DA, Pettit GR, Lippert III JW, Shnyder SD, Cooper PA, Bibby MC (2004) Comparative preclinical pharmacokinetic and metabolic studies of the combretastatin prodrugs combretastatin A4 phosphate and A1 phosphate. *Clin. Cancer Res.* **10:** 1446-1453.

Kong Y, Grembecka J, Edler MC, Hamel E, Mooberry SL, Sabat M, Rieger J and Brown ML (2005) Structure-Based Discovery of Boronic Acid Bioisostere of Combretastatin A-4. *Chemistry & Biology*, **12:** 1007-1014.

Lin CM, Singh SB, Chu PS, Dempcy RO, Schmidt JM, Pettit GR, Hamel E (1988) Interactions of tubulin with potent natural and synthetic analogs of antimitotic agent combretastatin: a structure-activity study. *Mol. Pharmacol*. **34:** 200-208.

Lippert JW (2006) Vascular disrupting agents. *Bioorg. Med. Chem.* **15:** 605–615.

Mealy NE, Lupone B, Balcell M (2006) Drugs under development for the treatment of breast cancer: combretastatin A-4 phosphate. *Drug. Fut.* **(31):** 547-548.

McGown AT, Fox BV (1989) Structural and biochemical comparison of the antimitotic agents colchicine, combretastatin-A4 and amphetinile. *Anti-Cancer Drug Des*. **3:** 249-254.

Omura T and Sato R (1964) The carbon monoxide binding pigment of liver microsomes. *J Biol Chem* **239:** 3137–3142.

Pettit GR, Singh SB, Niven ML, Hamel E, Schmidt JM (1987) Antineoplastic agent 124. Isolation, structure and synthesis of combretastatin-A1 and combretastatin-B1, potent new inhibitors of microtubule assembly, derived from *Combretum caffrum. J. Nat. Prod.* **50 :**119-131.

Pettit GR, Singh SB, Hamel E, Lin CM, Alberts DS, Garciakendall D (1989) Antineoplastic agent 145. Isolation and structure of the strong cell-growth and tubulin inhibitor combretastatin-A4 *Experientia* **45:** 209-211.

Pettit GR, Temple C, Narayanan VL, Varma R, Simpson MJ, Boyd MR (1995) Antineoplastic agents 322. Synthesis of combretastatin-4 prodrugs. *Anti-Cancer Drug Des*. **10:** 299-309.

Rustin GJS, Galbraith SM, Anderson H, Stratford M, Folkes LK, Sena L, Gumbrell L, Price PM (2003) Phase I clinical trial of weakly combretastatin A4 phosphate: Clinical and pharmacokinetic results. *J. Clin. Oncol.* **21:** 2815-282.

Stevenson JP, Rosen M, Sun W, Gallagher M, Haller DG, Vaughn D, Giantonio B, Zimmer R, Petros WP, Stratford M, Chaplin D, Young SL, Schnall M, O'Dwyer P (2003) Phase I trial of

the antivascular agent combretastatin A-4 phosphate on a 5-day schedule to patients with cancer: Magnetic resonance imaging evidence for altered tumor blood flow. *J. Clin. Oncol.* **21:** 4428-4438.

Stratford MRL, Dennis ML (1999) Determination of combretastatin A-4 and its phosphate ester pro-drug in plasma by high-performance liquid chromatography. *J. Chromatogr. B* **721:** 77-85.

Tozer GM, Prise VE, Wilson J, Locke RJ, Vojnovic B, Stratford MRL, Dennis MF, Chaplin DJ (1999) Combretastatin-A4 phosphate as atumor-vascular targeting agent : Early effects in tumors and normal tissues. *Cancer Res*. **59:** 1626-1634.

Tron GC, Pirali T, Sorba G, Pagliai F, Busacca S, Genazzani AA (2006) Medicinal chemistry of combretastatin A4: present and future directions. *J. Med. Chem.* **49:** 3033-3044.

Yu C, Shin YG, Chow A, Li Y, Kosmeder JW, Lee YS, Hirschelman WH, Pezzuto JM, Mehta RG, van Breemen RB (2002) Human, Rat, and Mouse Metabolism of Resveratrol. *Pharmac. Res.* **19:** 1907-1914.

FOOTNOTES

a) Financial support from Università degli Studi del Piemonte Orientale “Amedeo Avogadro” is gratefully acknowledged.

b) Giorgio Grosa - Dipartimento di Scienze Chimiche, Alimentari, Farmaceutiche e Farmacologiche and Drug and Food Biotechnology Center, Università degli Studi del Piemonte Orientale “A. Avogadro”, Largo Donegani 2, 28100 Novara, Italy.

tel +39 (0)321 375854 Fax 39 (0)321 375621

e-mail: grosa@pharm.unipmn.it

LEGENDS FOR FIGURES

Figures:

Figure 1. Structure of stilbenic vascular disrupting agents.

Figure 2. LC-DAD-UV of liver microsomal incubations: A) rat, B) human, C) control incubation.

Figure 3. UV spectra of CA-4.

Figure 4. Positive ion mode LC-ESI-MS/MS chromatogram of rat liver microsomal incubations. (Unlabeled peaks are matrix related).

Figure 5. Positive ion mode LC-ESI-MS/MS chromatogram of human liver microsomal incubations. (Unlabeled peaks are matrix related. In the TIC Full MS/MS 331 chromatogram peaks at 20.51 min and 24.55 min are related to possible quinone species; see text for further details).

Figure 6. Proposed scheme for CA-4 *in vitro* rat and human liver microsomal metabolism. (‡ metabolite lacking of reference standard; see text for further details).

DMD Fast Forward. Published on September 21, 2007 as DOI: 10.1124/dmd.107.016998
This article has not been copyedited and formatted. The final version may differ from this version.

Table

Compound	MW	Correlated Peak	MS $[M+H]^+$	MS/MS
30	332	**M1**	333	318-301(100%)-273-269-181-169-165
31	332	**M2**	333	318-301(100%)-273-269-181-169-165
5	302	**M3**	303	288-271(100%)-243
10	302	**M4**	303	288(100%)-271-243-167
11	302	**M5**	303	288-271(100%)-243-167
29	330	**M7**	331	316-303(100%)-300-299
28	330	**M8**	331	316-303(100%)-300-299

Table 1. Positive ion mode ESI-MS/MS data obtained from authentic standards of metabolites (M1, M2, M3, M4, M5, M7, M8) of CA-4.

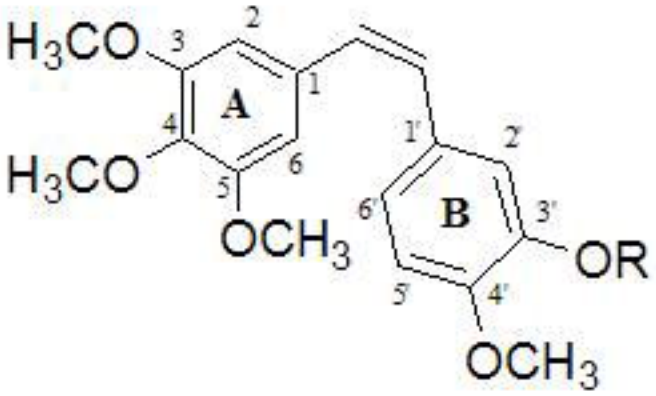

R= H; combretastatin A-4 **(CA-4) 1**

R= PO_3Na_2; (CA-4-P) **2**

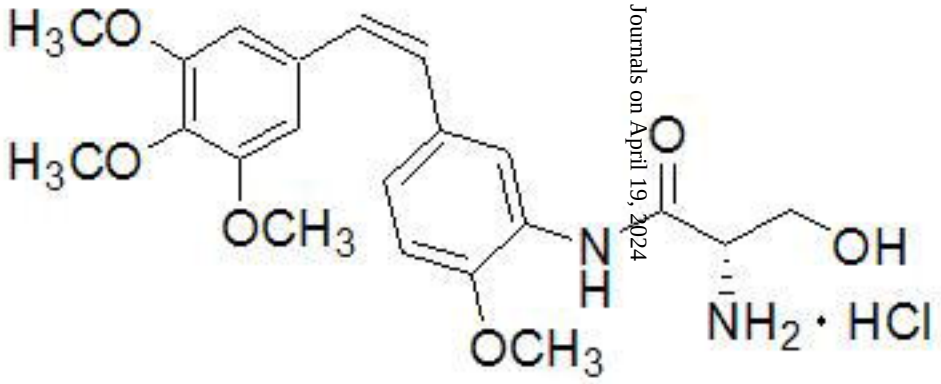

AVE8062 **3**

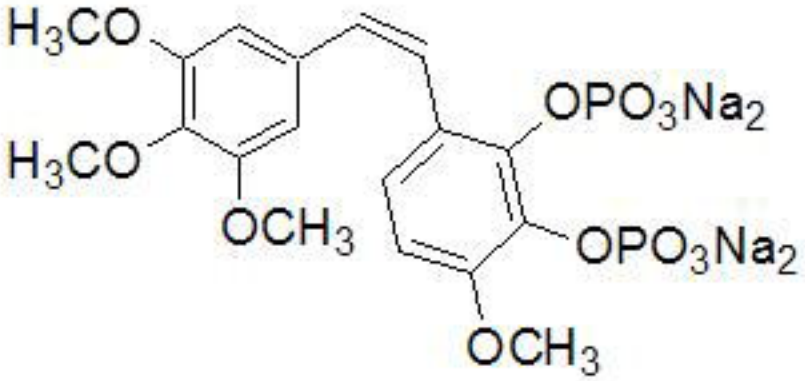

Oxi4503 **4**

Figure 1

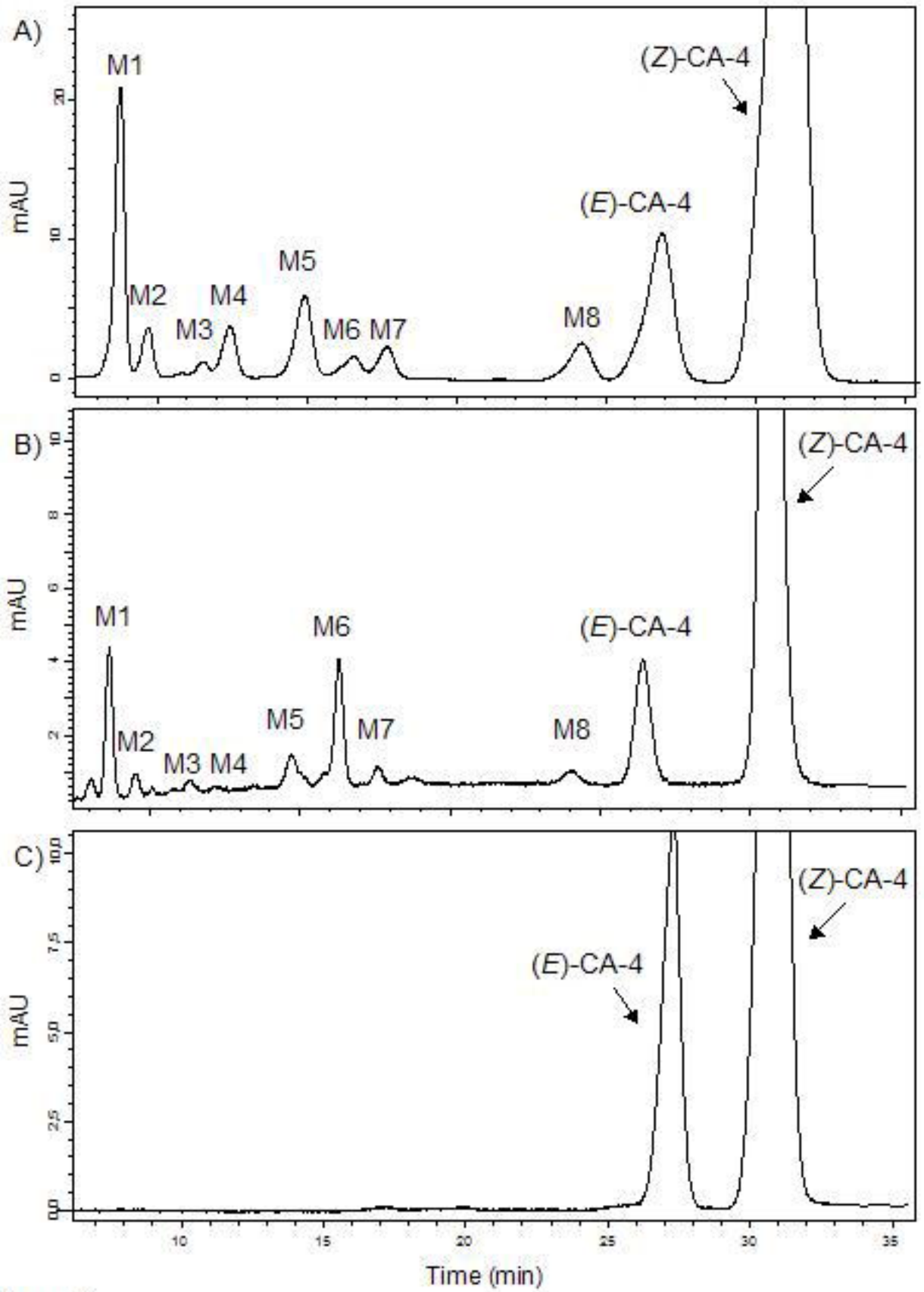
A)
M1
M2
M3
M4
M5
M6
M7
M8
(E)-CA-4
(Z)-CA-4
mAU
B)
M1
M2
M3
M4
M5
M6
M7
M8
(E)-CA-4
(Z)-CA-4
mAU
C)
(E)-CA-4
(Z)-CA-4
mAU
Time (min)

Figure 2

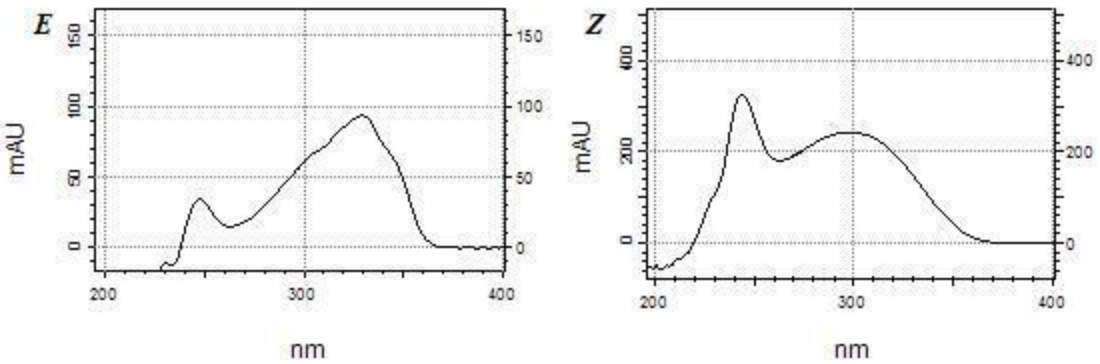

Figure 3

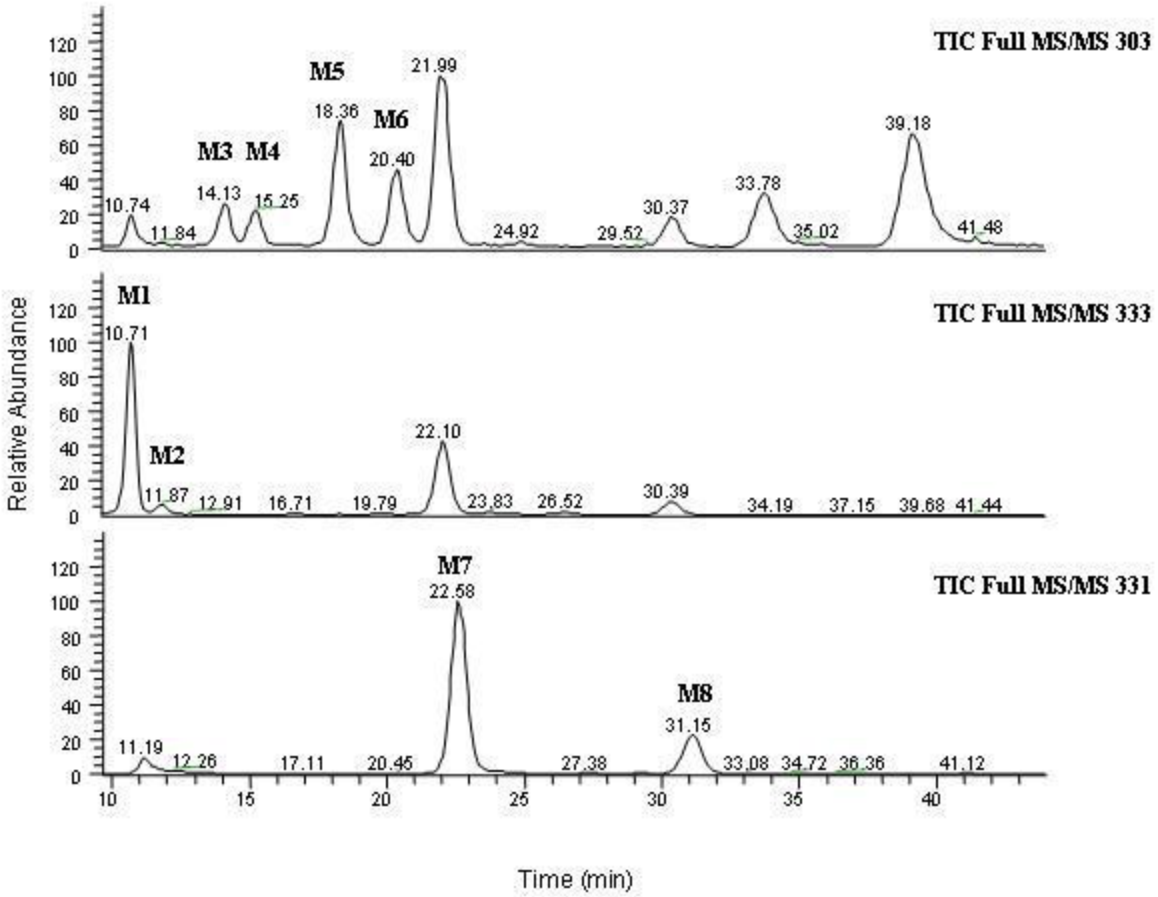
TIC Full MS/MS 303
M5
21.99
18.36
M6
M3 M4
20.40
14.13
15.25
10.74
11.84
24.92
29.52
30.37
33.78
35.02
39.18
41.48
TIC Full MS/MS 333
M1
10.71
M2
22.10
11.87
12.91
16.71
19.79
23.83
26.52
30.39
34.19
37.15
39.68
41.44
TIC Full MS/MS 331
M7
22.58
M8
31.15
11.19
12.26
17.11
20.45
27.38
33.08
34.72
36.36
41.12
Relative Abundance
Time (min)

Figure 4

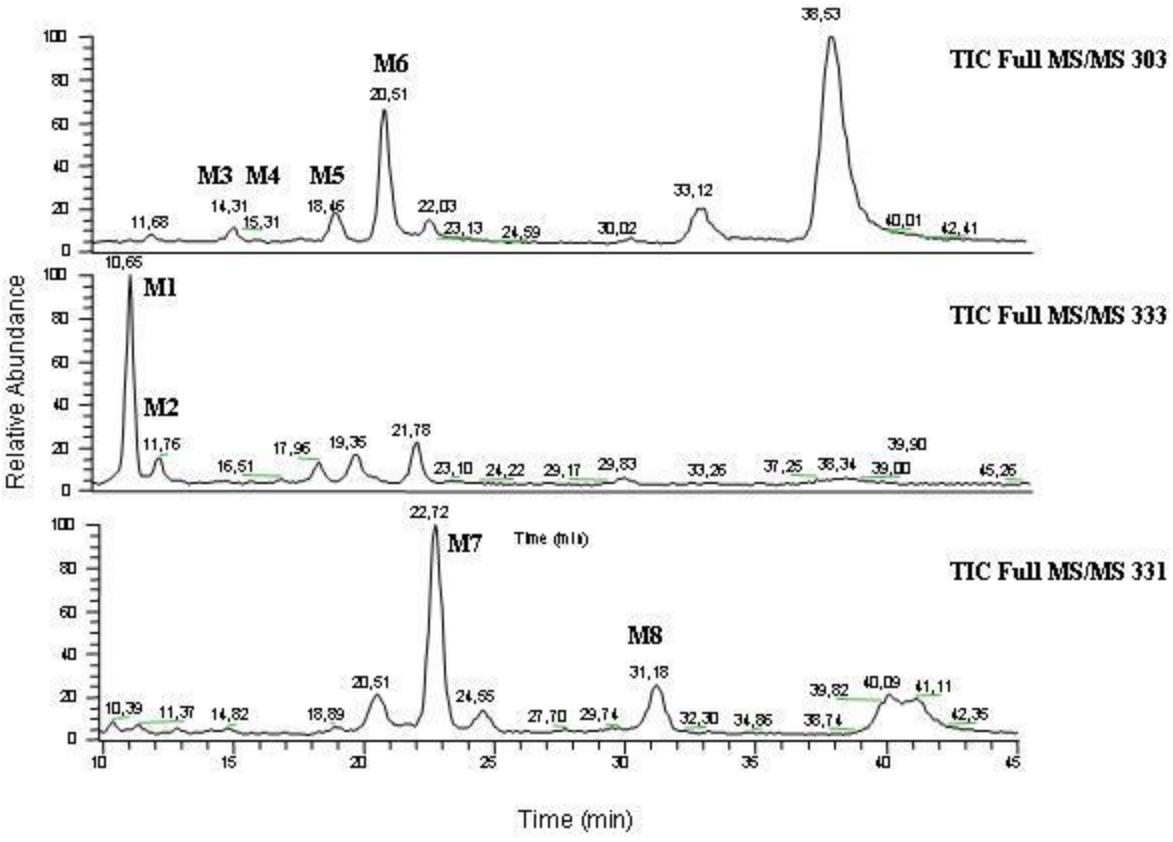
TIC Full MS/MS 303
TIC Full MS/MS 333
TIC Full MS/MS 331
M1
M2
M3
M4
M5
M6
M7
M8
Relative Abundance
Time (min)
Time (min)

Figure 5

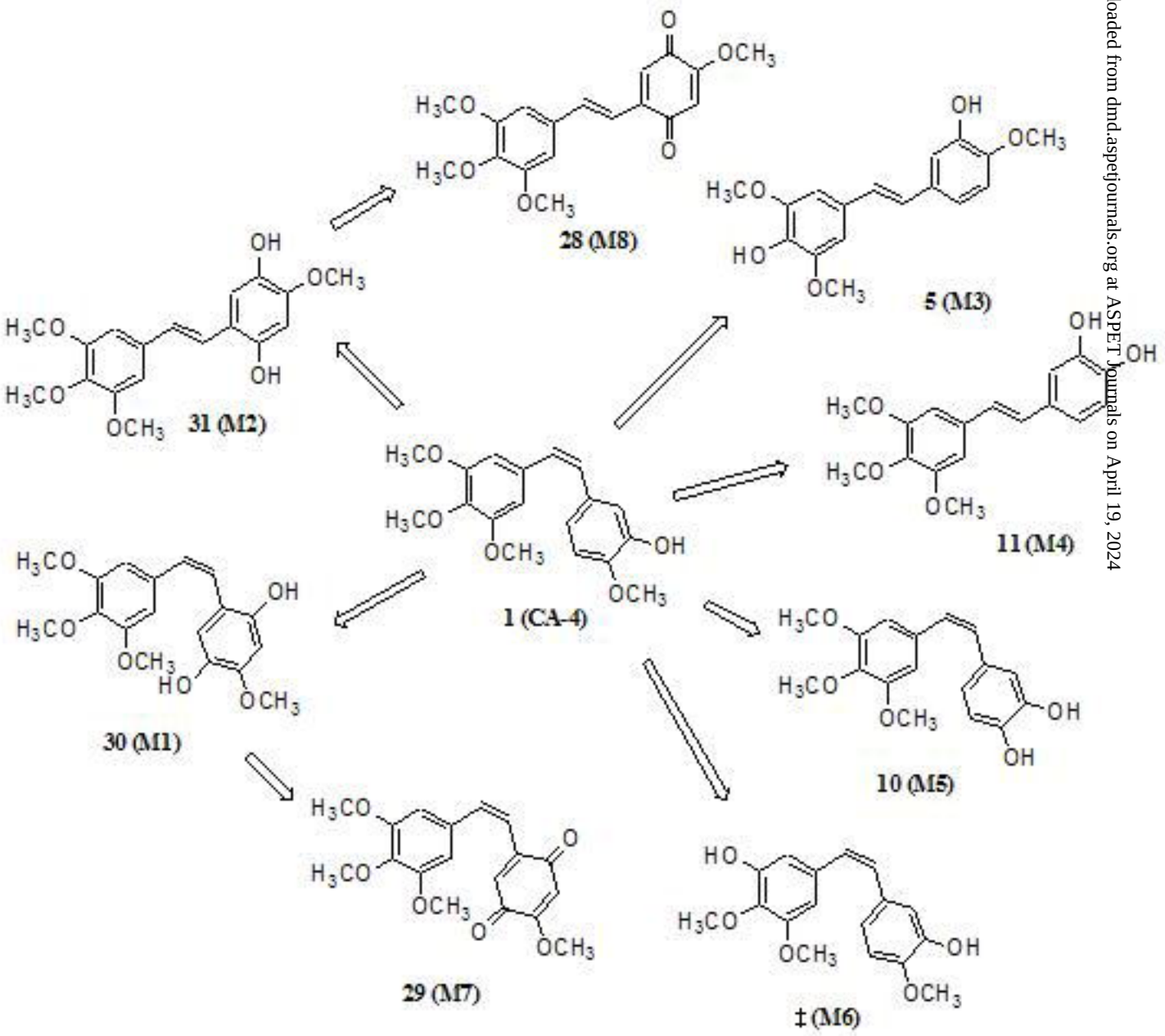

Figure 6